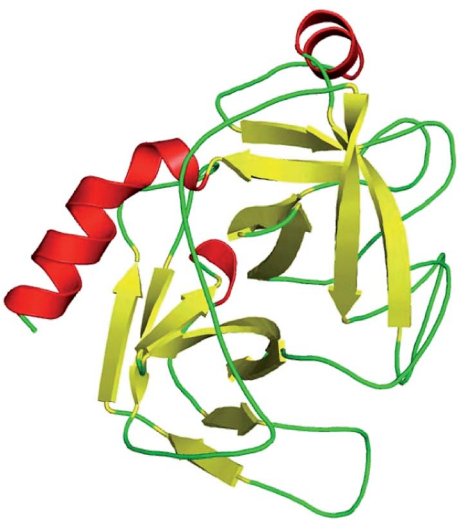

protein functional activities.[8 15] It is well-known fact that even a marginal change in the natural environment around the protein may cause adverse effects on its properties.[13] The co-solvent is often used by physical chemist or biochemist that either stabilizes or destabilizes the structures of biomolecules.[8,14 17] The biomolecule surface primarily interacts with the surrounding of solvent molecules that contributes to its folding/unfolding. Thus, the properties of the enzyme surface may be crucial for maintaining its catalytic active conformation in co-solvent. A more restrictive and specific term that will be employed the osmotic relationships of organisms is osmolyte.[8] The native conformation of the biomolecules under external osmotic stresses such as dehydration, temperature variations, variable pH, freezing, high salinity and internal stress such as high concentrations of protein denaturants can be stabilized by the osmotically active solutes, which are small organic molecules, termed as naturally occurring osmolytes.[8 25] These osmoregulatory compounds, referred to as protectants, tend to stabilize the protein structure without perturbing the biomolecule structure and function.[8,13 17]

The ability of urea and guanidine hydrochloride (GdnHCl) to denature the biomolecules has been extensively explored.[13 17,26 28] Proteins lose their definite compact structure and take up unfolded state with disorder in the backbone conformation in the presence of denaturants.[28 31] The denaturants shifts the folding equilibrium from the native state to partially unfolded, while opposite is true in the presence of osmolytes.[18,32] The stabilization of compact native structures reveal typically of preferential exclusion of osmolytes from the vicinity of the macromolecule surface. Energetically, unfavourable interactions may exist between osmolyte and hydration surfaces of protein.[26 28] On the other hand, denaturants can break the bonds within the protein and thus accumulate on the surface of protein through preferentially binding.[28 33]

Apparently, the influence of co-solvents on trypsin stability has not been quantified systematically. Here, we have focused on the isolation of trypsin from the digestive system of adult Indian major carp Catla *C. catla*. To gain further deeper insight into the structural aspects of trypsin, we have studied the stability of this biomolecule in the presence of osmolytes (TMAO, betaine and proline) and denaturants (urea and GdnHCl) by using several biophysical techniques and molecular dynamic (MD) simulation. Moreover, we have also estimated the Gibbs free energy of unfolding changes (ΔG_u) at 25 °C, which is a better indication of protein stability, from thermal analysis (T_m), enthalpy changes (ΔH) and heat capacity changes (ΔC_P).

2. Experimental section

2.1. Materials

Trypsin was extracted and purified by standard procedure[34] and the detailed procedure of extraction and purification is described in the ESI.† Fishes were maintained under standard living conditions and experiments were conducted with care. All experiments were performed in compliance with the relevant laws and institutional guidelines, Animal Ethical Committee, Department of Zoology, University of Delhi, Delhi and also the institutional committee(s) has approved the experiments. TMAO, betaine, proline, GdnHCl and Tris (hydroxymethyl) aminomethane from Sigma Chemical Co. and urea from Acros Organics were purchased. All chemicals are of analytical grade and used without further purification. Distilled deionized water with resistivity of 18.3 MΩ was used for the preparation of Tris–HCl buffer of 1.5 mM at pH 7.5. The concentration of protein was maintained at 3 mg mL^{-1} for all measurements.

2.2. Trypsin activity

Trypsin activity was measured with *N*-α-benzoyl-DL-arginine-*p*-nitroanalidine (BAPNA). 750 μL of BAPNA (1 mM in 50 mM Tris–HCl, pH 8.2, 20 mM $CaCl_2$) was incubated with 10 μL of enzyme extract at 37 °C and change of absorbance was recorded under kinetic mode for 3 min at 410 nm.[35] Trypsin activity was expressed as change in absorbance per min per mg protein of the enzyme used in the assay. Activity units were calculated by the following equation:

$$\text{Activity units} = \frac{(\text{Abs}_{410}/\text{min}) \times 1000 \times \text{mL of reaction mixture}}{\text{extinction coefficient of chromogen} \times \text{mg protein in reaction mixture}}$$

The molar extinction coefficient of *para*-nitroanalidine liberated from chromogens of BAPNA is 8800. Purified trypsin of Catla was incubated with various osmolytes such as TMAO, proline, betaine and denaturants such as urea and GdnHCl with concentrations ranging from 1 to 3 M. After incubating for 1 h in respective solutions then the percent relative activity of trypsin was determined according to Laemmli.[36]

2.3. Molecular study by SDS-PAGE

Separation of proteins in the enzyme extracts was done by 12% SDS-PAGE. Enzyme extract (20 μg protein per sample) was loaded onto each well and electrophoresis was performed (30 mA) on a vertical dual mini gel electrophoresis device (Hoefer SE-260, Amersham Pharmacia, Uppsala, Sweden) at a controlled temperature of 4 °C. The protein bands were studies by SDS-PAGE, samples containing 20 μg were loaded onto each well. After electrophoresis, the gel was then washed, stained with 0.1% Coomassie brilliant blue (CBB, Mumbai, India) in methanol : acetic acid : water (40 : 10 : 40) for 2 h. Destaining

was done with the same solution without CBB for 1 h. Clear bands were identified trypsin. The gels were documented in calibrated densitometer (GS-800, Bio-Rad, CA 94547, USA) with help of Quantity one – 4.5.1 software.

2.4. UV-Vis measurements

The absorption spectra of samples were recorded from 250 to 290 nm on a double beam spectrophotometer (UV-1800, SHIMADZU Co. Japan) equipped with 1.0 cm quartz cells at 25 °C.

2.5. Fluorescence spectroscopy

Fluorescence measurements were carried out on a Cary Eclipse fluorescence spectrophotometer (Varian optical spectroscopy instruments, Mulgrave, Victoria, Australia) with an intense Xenon flash lamp as light source. This instrument is equipped with a multi cell holder and Peltier device with precision of ±0.05 °C to operate sample at any desired temperature. The excitation wavelength set to 280 nm and slit widths of 5 nm for excitation and emission bandwidths, respectively. Thermal denaturation measurements of the sample were taken at a heating rate of 1 °C min^{-1}.

2.6. Circular dichroism (CD) spectroscopy

CD measurements were done with 1 cm path length rectangular quartz cell at 25 °C, on PiStar-180 spectrophotometer (Applied Photophysics, UK). This instrument is equipped with a Peltier system for controlling temperature of the sample cell at desired temperature. (1*S*)-(+)-10-Camphorsulfonic acid (Aldrich, Milwaukee, WI), which exhibits a 34.5 M cm^{-1} molar extinction coefficient at 285 nm, and 2.36 M cm^{-1} molar ellipticity (θ) at 295 nm, was used in calibration of the instrument. Each spectrum was collected in the range 196–250 nm by averaging six spectrums.

2.7. Molecular dynamics (MD) simulation

The crystal structure of trypsin was obtained from the protein databank (PDB ID: 2ptn).[37] The protonation state of trypsin structure is adjusted according to pH 8.2 using the H++ server employing the Poisson–Boltzmann equation.[38] The molecular dynamics (MD) simulation were performed using the GROMACS 4.5.5 package.[39] The standard GROMOS 53a6 force field[40] was used as the parameters for trypsin and co-solvents.

Table 1 Compositions of the simulated systems

	Number of molecules					
Systems	Tris	HTris	Ca^+	Cl	Water	Osmolyte/denaturant
50 mM buffer	6	5	5	21	11 447	
1 M betaine	6	5	5	21	9743	229
1 M proline	6	5	5	21	9874	229
1 M TMAO	6	5	5	21	10 190	229
1 M urea	6	5	5	21	10 671	229
1 M GdnHCl	6	5	5	250	10 109	229

The parameters of the force field for urea and GdnHCl are taken from Smith *et al.*[41] and Camilloni *et al.*[42] The parameters concerning TMAO, proline, and betaine were taken from the Automated Topology Builder (ATB) database.[43] The simulations were carried in explicit solvent using SPC/E water.[44] The enzyme was placed in a cubic box containing 1 M (betaine, proline, TMAO, urea, or GdnHCl), 50 mM Tris–HCl at pH 8.2, and 20 mM $CaCl_2$. The cubic box was large enough to contain trypsin and surrounded by 1 nm of solvent on all sides. The total charge of the simulation systems were neutralized with Cl counter-ions. The molecular numbers of the simulation systems are reported in Table 1. The number of molecules of neutral (Tris) and protonated ($HTris^+$) forms of 50 mM Tris–HCl was calculated based on its pK_a value (7.81)[45] using HySS (HYPERQUAD Simulation and Speciation) program.[46] The whole system was relaxed with 50 000 steps of the steepest descent energy minimization, which the maximum force on individual atoms was <1000.0 kJ mol^{-1} nm^{-1}. Prior to run production MD, each system was equilibrated for 500 ps in two phases, and the heavy atoms of the protein were restrained.

The first equilibration phase is to stabilize the temperature of the system with NVT ensemble at 300 K, whereas the second equilibration phase is conducted under an NPT ensemble to stabilize pressure of the system at 1 bar. The position restraints of protein were finally released and the system was equilibrated for 20 ns (10 000 000 steps) at constant temperature and pressure (NPT ensemble), in the production MD phase, for data collection. The MD simulations were performed using MD Leapfrog integrator with a time step of 2 fs. The cut-off of the short-range Coulombic and Lennard-Jones (LJ) interactions was 1.0 nm. The long range Coulombic interactions were treated with Particle-Mesh Ewald (PME) method with a Fourier spacing of 0.16 nm and an interpolation order of four.[47] The chemical bonds to hydrogen atoms were constrained with the LINCS algorithm.[48] Temperature and pressure of the simulation system were controlled by velocity-rescaling thermostat[49] and Parrinello and Rahman barostat,[50] respectively. The coordinates of the 20 ns trajectory were saved every 2 ps for analysis. GROMACS 4.5.5 package has several tools for analysis the simulation trajectories. The g energy tool was used to calculate the electrostatic and Lennard-Jones energies between the pairs. The g gyrate tool was used to compute the radius of gyration of protein. The number of the hydrogen bonds between trypsin and solutes was calculated using g hbond tool with donor–acceptor distances of less than 0.35 nm and a cut-off angle (acceptor–donor–hydrogen) less than 30°. The g rdf tool was used to calculate the radial distribution functions and coordination numbers between particles. The molecular structures and snapshots were visualized using the visual molecular dynamics (VMD) software.[51]

3. Results and discussion

3.1. Effect of co-solvents on the activity of trypsin

Trypsin was treated with different co-solvents and the relative activity of trypsin was determined in percentage. The activity of purified trypsin was treated as 100% for comparison with that

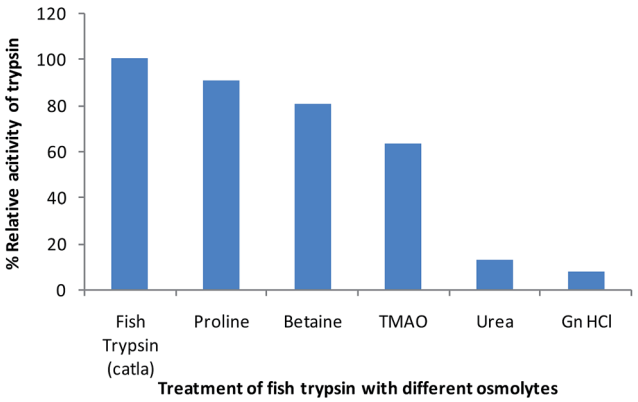

Fig. 2 Percent relative activity of purified trypsin, *Catla catla* with 1 M concentration of different co-solvents such as TMAO, proline, betaine, urea and GdnHCl.

in different co-solvents. The obtained activity results of trypsin in different co-solvents were displayed in Fig. 2. The trypsin was found with 90.5% relative activity in the presence of proline as shown in Fig. 2. The relative activity of trypsin was found to be 80.5 and 63.1, in the presence of betaine and TMAO, respectively. On the other hand, not surprisingly trypsin was completely lost its activity in the presence of urea and GdnHCl.

3.2. Study of the behaviour of trypsin at molecular level in the presence of co-solvents

To evaluate the binding capability of co-solvents to trypsin structure, we used gel electrophoresis and the obtained results were summarized in Fig. 3. Folding and unfolding of protein have been observed with the help of banding pattern obtained from the SDS-PAGE.[52 54] Baldwin *et al.*[52] focused on the folded and unfolded proteins on SDS-PAGE and used to quantitate their unfolding.

According to Dewald *et al.*[54] SDS-PAGE mobility assay allows the discrimination of aggregate, unfolded membrane associated and folded membrane associated protein state. In our study, SDS-PAGE was performed to explore the alterations in protein by observing the banding pattern with reference to control (buffer). SDS is a strong agent used to denature native proteins to unfolded state, individual polypeptides. In this process, the intrinsic charges of the polypeptides become negligible as compared to the negative charges contributed by SDS.

The results in Fig. 3 shown that proline (P), betaine (B), TMAO (TM) and urea (U), at concentration of 1 M, stabilized the conformation of trypsin. However, the conformation was completely unfolded with the addition of GdnHCl at 1 M and 2 M GdnHCl as shown in Fig. 3. Surprisingly, the trypsin conformation was partially disturbed in the presence of proline, betaine, TMAO and urea at 2 M. The structure was completely denatured in the all investigated co-solvents at the concentration of 3 M. Similar study was conducted by Dewald *et al.*[54] in which there was the spontaneous folding of two Neisserie outer membrane proteins by the addition of urea. These results have confirmed that the change in folded conformation of trypsin can be varied depend upon the nature of the co-solvent. These differences in conformation of trypsin in response to different co-solvents can be understood from the protein water-accessible surface area (ASA).[55] Denaturants, such as urea is known to enhance the ASA of the protein and thereby protein structure was altered, whereas reverse was true for TMAO and betaine.[55]

3.3. Understanding of folding and unfolding states of trypsin in the presence of co-solvents by thermodynamic parameters

Thermodynamic parameters are evolved as paradigm to understand the protein folding and unfolding.[8,13] Transition temperature (T_m), Gibbs free energy change (ΔG) and enthalpy change (ΔH), among others, play a great role in delineating the noncovalent forces that involve in stabilizing the different structural features of the biomolecules.[56] T_m, ΔG and ΔH were determined from temperature dependent fluorescence intensity curves as shown in Fig. 4 and obtained data collected were

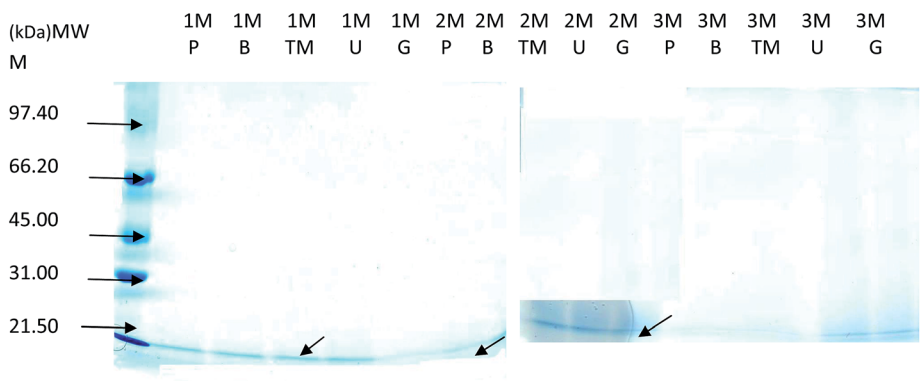

Fig. 3 SDS-PAGE of purified trypsin of *Catla catla* treated with various co-solvents proline (P), betaine (B), TMAO (TM), urea (U) and GdnHCl (G) with concentrations ranging from 1 to 3 M, respectively. Sample was diluted (1 : 1) with sample buffer. MWM comprising phosphorylase b (97 400); bovine albumin (66 200); ovalbumin (45 000); carbonic anhydrase (31 000); and trypsin inhibitor (21 500). After electrophoresis the gel was directly stained with Coomassie brilliant blue R-250 for 2 h and destained. M Bio Rad Marker low range.

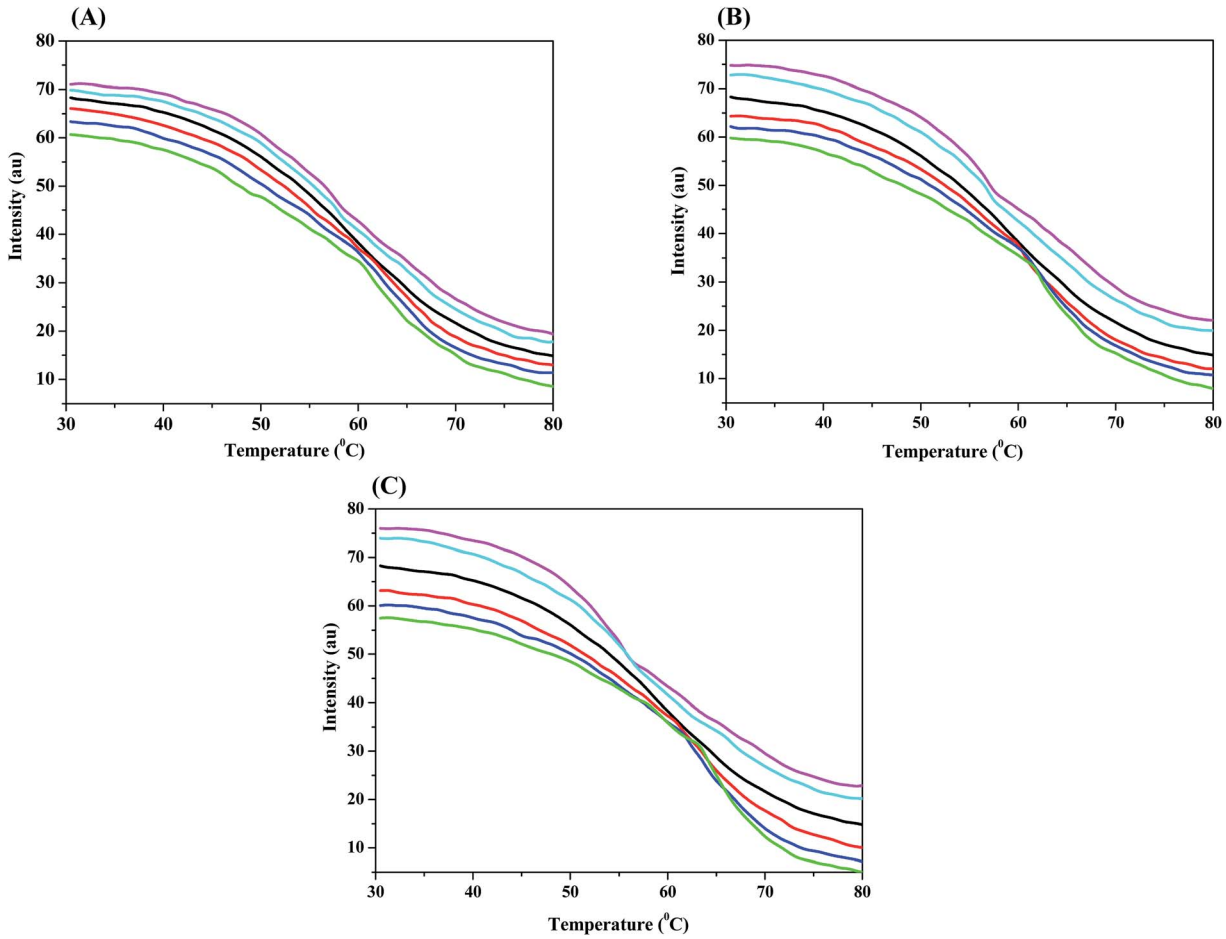

Fig. 4 Temperature dependent fluorescence intensity of trypsin in various co-solvents at different concentrations: (A) 1 M, (B) 2 M and (C) 3 M. Colour lines represent buffer (black line), TMAO (red line), proline (blue line), betaine (green line), urea (cyan line) and GdnHCl (magenta line).

shown in Table 1S.† A sigmoidal type of fluorescence intensity curves were obtained for trypsin in the presence and absence of co-solvents. The values of map N and map D for the protein were obtained through linear fitting of the pre- and post-transition data.[57,58] The Gibbs energy of unfolding at 25 °C (ΔG_u) has been calculated by using the following equation,

$$\Delta G_u(T) = \Delta H[1 \quad (T/T_m)] \quad \Delta C_P[(T_m \quad T) + T \ln(T/T_m)] \quad (1)$$

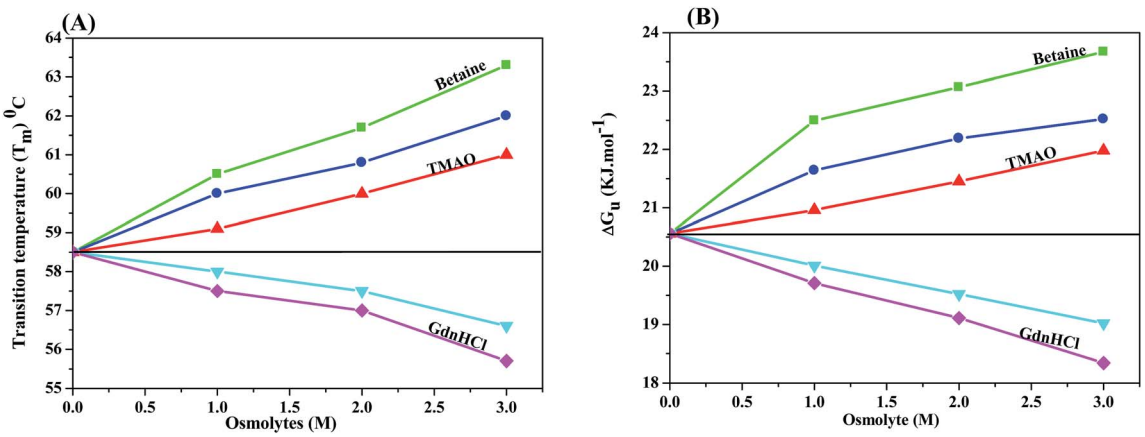

Fig. 5 (A) Transition temperature (T_m) and (B) calculated Gibbs free energy changes in unfolding state (ΔG_u) at 25 °C for the trypsin in different solvent media. Colour lines represent buffer (black line), TMAO (red line), proline (blue line), betaine (green line), urea (cyan line) and GdnHCl (magenta line).

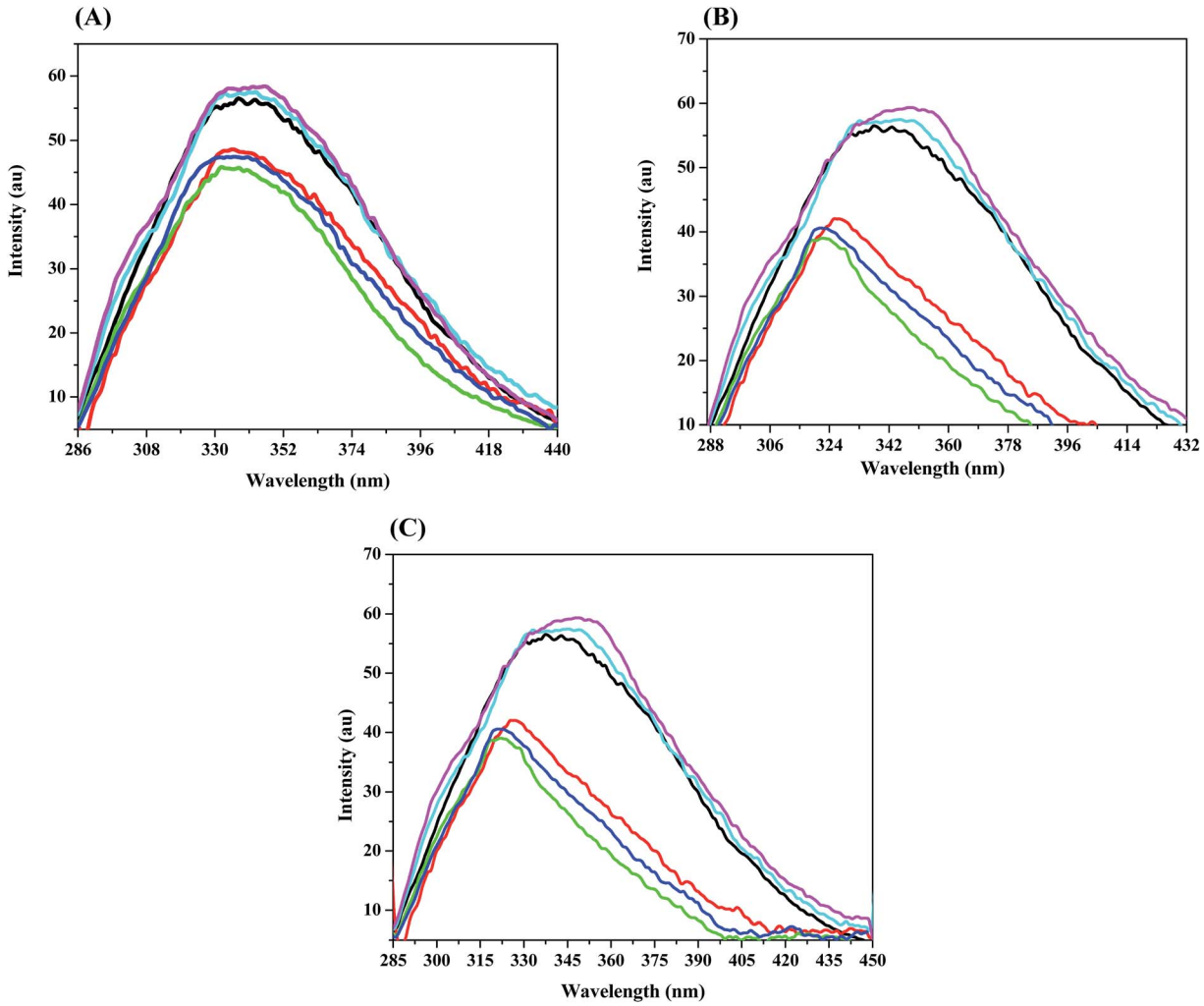

Fig. 6 Fluorescence intensity of trypsin in various co-solvents at different concentrations: (A) 1 M, (B) 2 M and (C) 3 M. Colour lines represent buffer (black line), TMAO (red line), proline (blue line), betaine (green line), urea (cyan line) and GdnHCl (magenta line).

From Table 1S† and Fig. 5A, one can observe that the T_m values were rapidly increased with addition of osmolytes (from 58.5 °C (in the buffer) to 63.3, 62.0 and 61.0 °C in the presence of 3 M betaine, proline and TMAO, respectively), while the T_m values were decreased with the addition of the denaturants (from 58.5 °C (in the buffer) to 56.6 and 55.7 °C in the presence of 3 M of urea and GdnHCl, respectively). Out of three stabilizers, betaine proved to be the strongest stabilizer, whereas, proline and TMAO were moderate and weak stabilizers, respectively, for protecting the protein folded conformation. The stabilizing abilities of different stabilizers for native state of trypsin varied from stabilizer to stabilizer; therefore, the efficiency of stabilizing effects of stabilizers follows the trend: betaine > proline > TMAO. On the other hand, GdnHCl proved to be the stronger destabilizer for the trypsin folded conformation. It is worth noting that the T_m values were increased with increasing the concentration of all the stabilizers, conversely, the T_m values were decreased with increasing the concentrations of denaturants. The preferential hydration of protein in the presence of stabilizers can enhance the stability of proteins.[59 63]

The profile of ΔG_u in buffer and in the presence of different co-solvents, were obtained for trypsin by using the eqn (1) and displayed in Fig. 5B and tabulated in Table 1S.† The results in Fig. 5B and Table 1S† show that the values of ΔG_u were increased linearly with the concentration of osmolytes indicating that trypsin was stabilized by the stabilizers. On the other hand, addition of denaturants to the protein led to decrease in ΔG_u values. Betaine has shown large stabilizing effects on trypsin as indicated by elevated ΔG_u value (23.67 kJ mol^{-1} in 3 M betaine solution) compared with control (20.56 kJ mol^{-1} in buffer). In addition to betaine, the remaining two stabilizers, proline and TMAO, show stabilizing effects on trypsin as it was evidenced from the enhancement in the ΔG_u values (22.52 and 21.98 kJ mol^{-1} in 3 M proline and TMAO, respectively). In contrast, trypsin has shown the ΔG_u value of 18.34 kJ mol^{-1} in 3 M GdnHCl, which shown that the native structure of trypsin was perturbed.

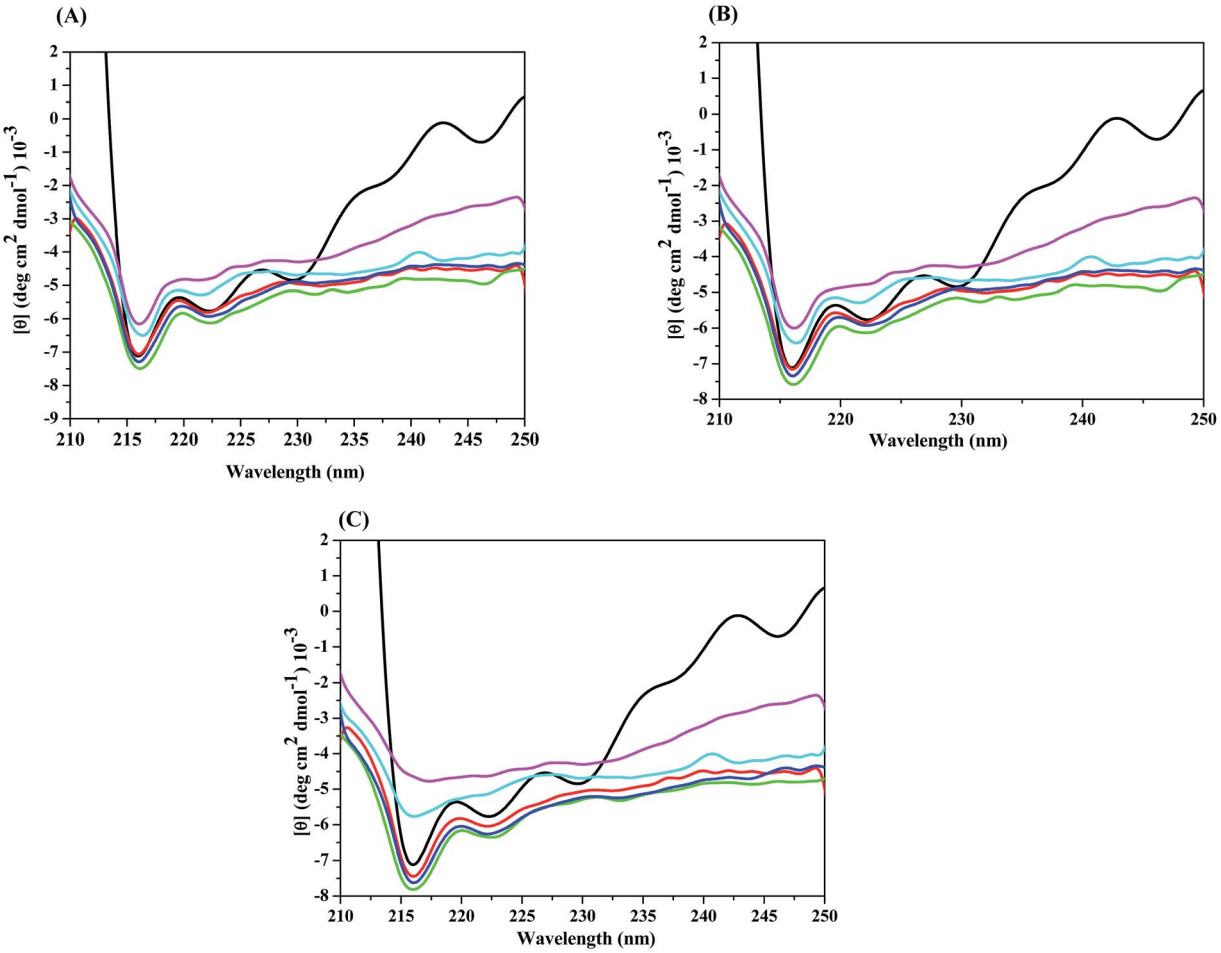

Fig. 7 Far-UV CD spectra of trypsin in various co-solvents at different concentrations: (A) 1 M, (B) 2 M and (C) 3 M. Colour lines represent buffer (black line), TMAO (red line), proline (blue line), betaine (green line), urea (cyan line) and GdnHCl (magenta line).

Further, the enhancement in concentration of stabilizers leads to a drastic decrease in protein surface area and thereby decreasing the configurational entropy of the unfolded state. This view provides a rationale for expecting an entropy decrease in the native ↔ unfolded equilibrium in the presence of the stabilizers when compare to the equilibrium in the absence of stabilizers. As tabulated in Table 1S,† the ΔH and ΔC_P values of trypsin in all three stabilizers were positive and obviously higher than the control point. Altogether, the results indicate that stabilizers interact unfavorably with the surface of trypsin while the denaturants interact favorably with surface of trypsin.

3.4. Steady state fluorescence spectroscopy

Using the fluorescence spectroscopy for assessing the stability profile of proteins in the presence of co-solvents is a very important characterization and quality control step for any biopharmaceutical.[64] The prerequisite for implementation of fluorescence spectroscopy in protein studies is the presence of fluorophore or fluorochrome. In trypsin, four tryptophans (Trp 51, Trp 141, Trp 215, and Trp 237) are considered as an intrinsic fluorophores.[64,65] The fluorescence spectra of trypsin in different co-solvents were displayed in Fig. 6A. As shown in Fig. 6A, trypsin has exhibited a strong fluorescence emission at about 340 nm in buffer solution. The peak at 340 nm has exhibited blue shift in emission wave length upon addition of stabilizers (betaine, proline and TMAO), whereas, this peak has shown red shift in emission wavelength over the addition of the denaturants (urea and GdnHCl).

The fluorescent (Trp), hydrophobic group, has been buried with the addition of stabilizers in such a way that it is coming closer to sulphur containing groups such as Cys and disulphide bonds which can act as efficient quencher of Trp fluorescence. This is leading to decrease in fluorescence intensity. In contrast to this, these hydrophobic groups were exposed as the protein unfolds by the addition of denaturants and lead to the high fluorescence emission intensities.[61] The intensities were decreased with enhancement of osmolytes concentration, while intensities were gradually increased with enhancement of denaturant concentration (Fig. 6B and C). The enhancement of fluorescence intensities in the high concentration of denaturants suggest that the tryptophans have moved further away from sulfur containing groups such as cysteine and disulfide bond which can act as an efficient quenchers of tryptophan fluorescence in native state.[66,67] This is due to the fact that the

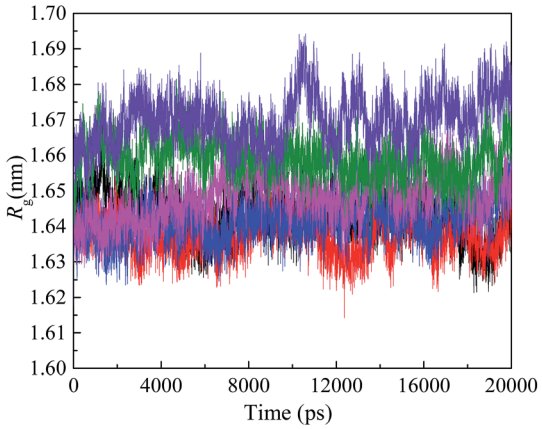

Fig. 8 Variations in R_g of trypsin with time for 20 ns in buffer (black line), 1 M betaine (red line), 1 M proline (blue line), 1 M TMAO (magenta line), 1 M urea (olive line), and 1 M GdnHCl (violet line).

quantum yield of tryptophan in proteins is difficult to predict. Several amino acid side chains, as well as the peptide bond, are efficient quenchers of tryptophan fluorescence through excited-state proton or electron transfer.[68,69]

3.5. Circular dichroism spectroscopy

CD has been proved an excellent spectroscopic technique for monitoring protein folding and unfolding states that are induced by the various factors.[70] The CD spectrum in the far-UV region can provide information about the nature and composition of different secondary structural elements such as α-helices, β-sheets, turns, and random coils in a protein.[71] The far-UV CD spectra for trypsin in the presence of co-solvents (1 M) have been shown in Fig. 7A. The protein containing an α-helix exhibits two negative bands at 208 and 222 nm in the far UV-CD spectra. Also, a negative band between 210 and 222 nm resembles protein β-sheet. As Fig. 7A has reflected that the enhancement of magnitude of negative sign of two bands at 216 and 222 nm with the addition of osmolytes, whereas the reverse was true for denaturants. The decrease in the magnitude of negative ellipticity of bands at 216 and 222 nm with addition of denaturants indicated that the drop in helical content and an increase in β-turn and random coil content. Further, the decrease in the magnitude of negative signs of bands at 216 and 222 nm was more pronounced with addition of GdnHCl.

On the other hand, the enhancement of negative ellipticity of two bands at 216 and 222 nm was significantly pronounced by the addition of betaine and thereby, secondary structure of protein was enhanced. However, the trends in two bands at 216 and 222 nm in the presence of proline or TMAO were very similar to that of betaine. The enhancement or diminishment in the magnitude of negative signs of the bands was further pronounced with increasing the concentration of co-solvents (Fig. 7B and C). The increase in the concentration of stabilizers in bulk buffer leads to the utilization of more water molecules in solubilization process and thereby competition starts for the available water between proteins and solutes.[72] Due to this competition there is a reduction in the protein solvation layer, which results in a decrease in the apparent molal volume of the protein. As a result, the protein becomes more compact in the presence of stabilizers and finally leads to the more magnitude of negative ellipticity at 216 and 222 nm. Therefore, our results have shown the evidence of conformational changes of trypsin in the presence of various co-solvents.

3.6. Molecular dynamics (MD) simulation

The radius of gyration (R_g) as a function of time is an important tool to illustrate the spreading of the protein structure out of from its center. In Fig. 8, the R_g of trypsin in 1 M of the co-solvents varying with time were plotted. This figure has suggested that the enzyme structure remains unchanged during the simulations. The R_g show that the co-solvents, at 1 M, have no significantly different effects on the enzyme structure. The enzyme structure in the stabilizers solution was more stable and compact structure than that in the denaturant solution, which the R_g follows the trend: betaine < proline < TMAO < urea < GdnHCl.

The electrostatic (Coulomb) and the van der Waals (Lennard-Jones) interaction energies of solute–water and enzyme–solute pairs were calculated from the MD simulations and reported in Table 2. The interaction energies between stabilizers and water were negative and follow the order betaine > proline > TMAO. The electrostatic and the van der Waals energies between the osmolytes and trypsin were also negative and have the order proline ≥ betaine > TMAO; however, they are much smaller than those between the stabilizers and water. Thus, the stabilizer enhances the water structure and reduces the enzyme–water interactions, which could be associated with its ability to protect protein native structure. The interaction energies of

Table 2 The Coulomb and the Lennard-Jones energies of solute water and enzyme solute pairs obtained from the MD simulation

	$E_{Coulomb}$/(kJ mol ^{1})		$E_{Lennard\text{-}Jones}$/(kJ mol ^{1})		$E_{(Coulomb+Lennard\text{-}Jones)}$/(kJ mol ^{1})	
Solutes	Solute water	Trypsin solute	Solute water	Trypsin solute	Solute water	Trypsin solute
Betaine	58 920.7 ± 200.0	2030.6 ± 61.0	3153.2 ± 16.0	748.8 ± 34.0	62 073.9	2779.4
Proline	51 156.2 ± 190.0	1974.4 ± 74.0	2603.2 ± 10.0	835.4 ± 30.0	53 759.4	2809.8
TMAO	27 442.7 ± 52.0	1061.2 ± 30.0	3047.4 ± 9.6	672.5 ± 19.0	30 490.1	1733.7
Urea	22 246.8 ± 50.0	873.0 ± 41.0	2359.3 ± 6.1	483.4 ± 19.0	24 606.1	1356.4
GdnHCl	27 515.5 ± 58.0	1329.1 ± 98.0	2217.0 ± 4.0	119.2 ± 3.5	25 298.5	1448.3

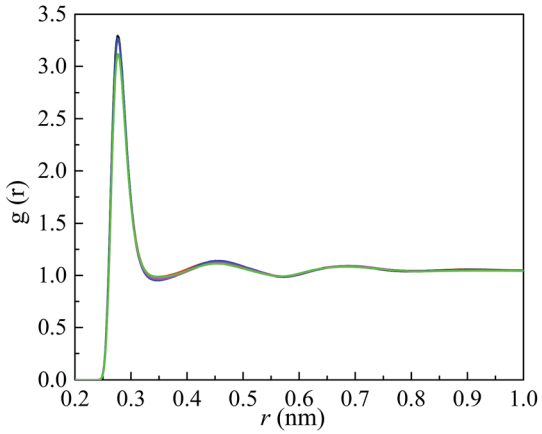

Fig. 9 The radial distribution function (RDF) between water oxygen atoms (OW OW) in 1 M betaine (black line), 1 M proline (red line), 1 M TMAO (blue line), 1 M urea (pink line), and 1 M GdnHCl (green line). The curves of betaine, proline, and TMAO overlap on each other; and the urea and GdnHCl are also overlapping.

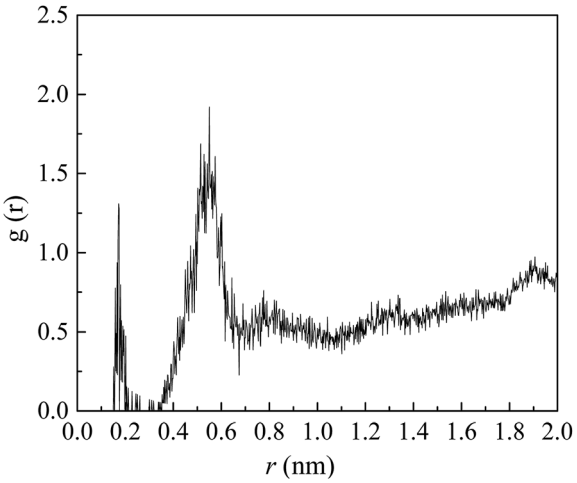

Fig. 11 The (SER195:HG···TMAO:O) RDF obtained from MD simulations of trypsin in 1 M TMAO.

trypsin–GdnHCl are greater than those of trypsin–urea. The electrostatic energy between GdnHCl and water is higher than that of urea–water, while the van der Waals energy of the latter is higher than the former that shows a positive value. To examine the effect of the osmolytes and denaturants on the water structure, the radial distribution function (RDF) between water oxygen atoms (OW) were calculated from the simulation results and plotted in Fig. 9. The RDF provides quantitative information of enhancement or lessening of density and arrangement of atom around the other atom. The peak of the (OW–OW) RDF (at 0.27 nm) in the presence of the osmolytes is higher than that of the denaturants. This suggests that the osmolytes enhance the hydrogen bonding between water molecules, and therefore strengthening the water structure and stabilising the enzyme structure.

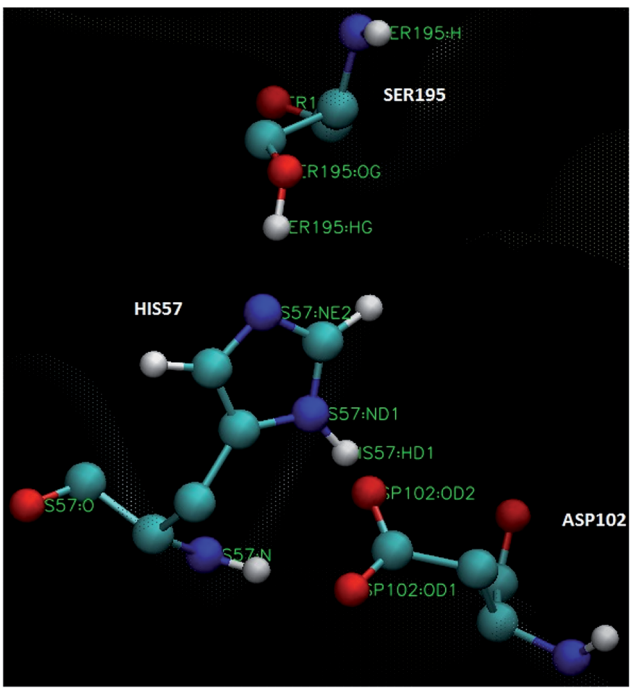

Fig. 10 Schematic diagram of the active site of trypsin.

Hydrogen bond formations between protein and solutes are important for the structural stability of the protein. The average number of hydrogen bonds $\langle N_{HB} \rangle$ between trypsin and co-solvents is calculated from MD simulations. The $\langle N_{HB} \rangle$ values for proline, betaine, TMAO, urea, and GdnHCl with trypsin are 35.04, 26.37, 17.83, 39.79, and 31.49, respectively. To understand the effect of these co-solvents on trypsin activity, the hydrogen bond formations between the co-solvents and the active site of trypsin were investigated. The catalytic triad of trypsin consists of the residues SER195, HIS57, and ASP102, which they are close to each other, as shown in Fig. 10. The hydroxyl group of the residue SER195 forms a covalent bond with the substrate. HIS57 residue accepts the hydroxyl's proton of SER195 (SER195:HG) to facilitate formation of the covalent bond. The role of ASP102 is to stabilize the positive charge of HIS57. By the inspection the hydrogen bonds formation between the studied solutes and the catalytic triad, TMAO, urea, and GdnHCl were found to form hydrogen bonds with the active site residues, whereas betaine and proline are not. TMAO was found to form hydrogen bond with active proton of SER195 (HG); consequently, it seems that this interaction is responsible for the decrease in the enzyme activity. The RDF of the oxygen atom of TMAO and SER195:HG, as shown in Fig. 11, has a peak at 0.16 nm which related to the hydrogen bond between them. A variety of hydrogen bonds was found between the hydrogens of GdnHCl with SER195:OG, SER195:O, HIS57:NE2, and HIS57:ND1. Fig. 12 shows the RDFs for the hydrogen bond sites of GdnHCl and these residues, and the result reveals that the RDF of SER195:OG is higher than SER195:O and the RDF for HIS57:NE2 is higher than HIS57:ND1. Urea was also formed several hydrogen bonds with SER195:H, SER195:OG, HIS57:O, HIS57:NE2, and HIS57:ND1, and the corresponding RDFs are plotted in Fig. 13. Both the hydrogen and oxygen atoms of urea

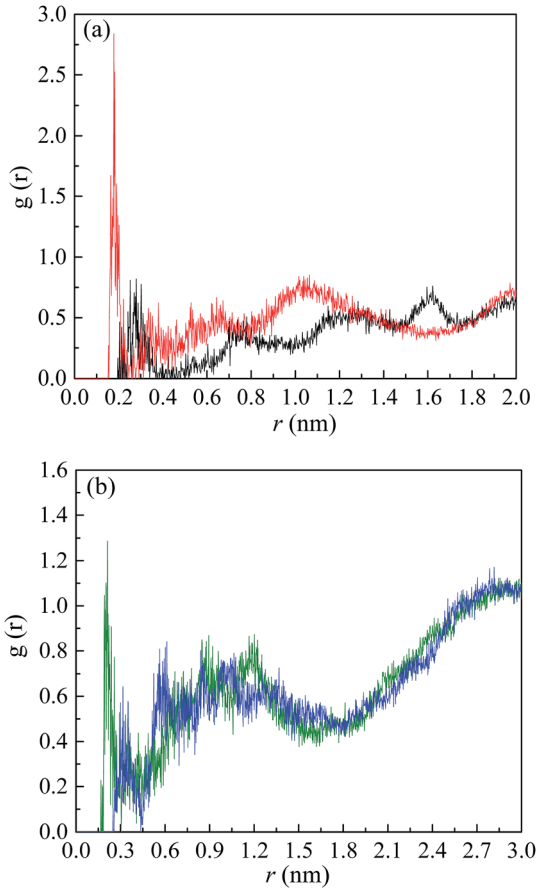

Fig. 12 The RDFs of GdnHCl SER195 (a) and GdnHCl HIS57 (b) interactions obtained from MD simulations of trypsin in 1 M GdnHCl; (SER195:O···GdnHCl:H) black line, (SER195:OG···GdnHCl:H) red line, (HIS57:NE2···GdnHCl:H) green line, and (HIS57:ND1···GdnHCl:H) blue line.

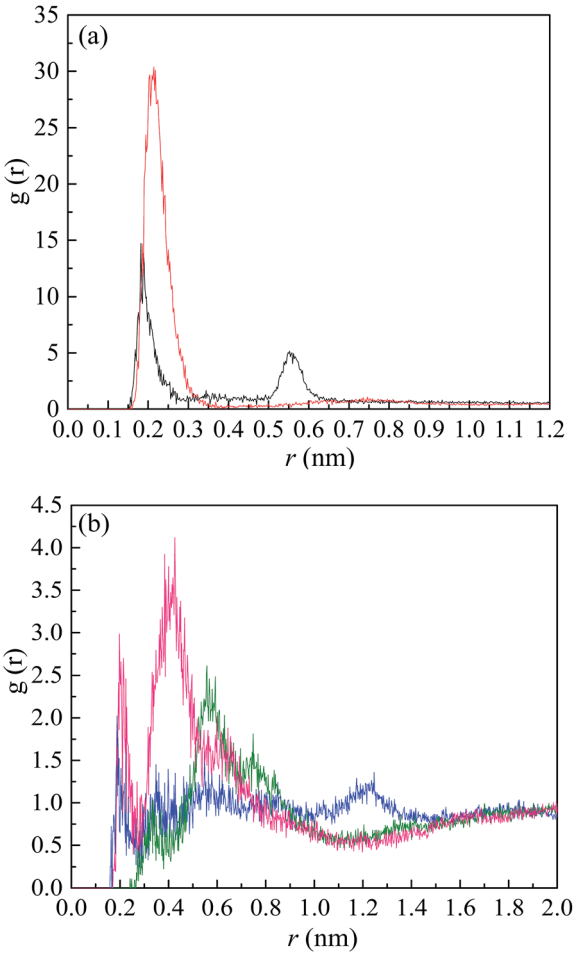

Fig. 13 The RDFs of urea SER195 (a) and urea HIS57 (b) interactions obtained from MD simulations of trypsin in 1 M urea; (SER195:OG···urea:H) black line, (SER195:H···urea:O) red line, (HIS57:O···urea:H) blue line, (HIS57:ND1···urea:H) olive line, and (HIS57:NE2···urea:H) pink line.

were able to form hydrogen bonds with the active site. The (urea:O···SER195:H) and (urea:H···SER195:OG) RDFs show sharp peaks appear at (0.21 and 0.18) nm, respectively. The (urea:H···SER195:NE2), (urea:H···SER195:O), (urea:H···SER195:ND1), RDFs exhibit peaks corresponding to their respective hydrogen bonds at (0.20, 0.19, and 0.33) nm. The urea molecules located near to the protein surface are shown in Fig. 14A, as an example, which indicate their direct interaction. For instance, Fig. 14B shows the hydrogen bond formation between (urea:H···SER195:OG). It is clear from the MD simulation that the significant decrease in trypsin activity in 1 M denaturant solution is mainly due to the hydrogen bonds between the denaturant and the catalytic triad.

Overall, our results have strongly delineated that the stability of trypsin was enhanced by increasing the concentration of stabilizers, while the stability was decreased as increasing the concentration of denaturants. Our experimental and MD simulation results have clearly explained that the stabilizers have increased the stabilization of trypsin in the order: betaine > proline > TMAO. The weak stabilizing ability of TMAO was mainly due to the weak unfavourable interaction between TMAO and trypsin functional groups as it was reflected from the lower ΔG_u of trypsin in the presence of TMAO. Interestingly, the ΔG_u values of trypsin in the presence of different stabilizers show that betaine was the strongest stabilizer, while proline was a moderate stabilizer and TMAO was a weak stabilizer. The present trend of stabilizers was quite interesting and surprising. Indeed, TMAO acts as a strongest stabilizer for various biomolecules.[13 18,26,60] However, in the present study TMAO proved to be a weakest stabilizer. Analogously, a similar phenomenon was observed by Bruździak *et al.*[73] According to Bruździak *et al.*, TMAO has acted as a weak stabilizer for hen egg white lysozyme. Further, Canchi *et al.*[74] have also revealed through simulations that TMAO cannot act as a protectant for stable conformation of proteins and may even acted as a denaturant.

Our results have shown that the stabilizers were excluded from water molecules around trypsin structure and thereby and thereby, the protein has adopted more compact conformation. The present results are corroborated with the recent experimental results[73,75 78] in which the globular proteins do not undergo any conformational changes in the presence of

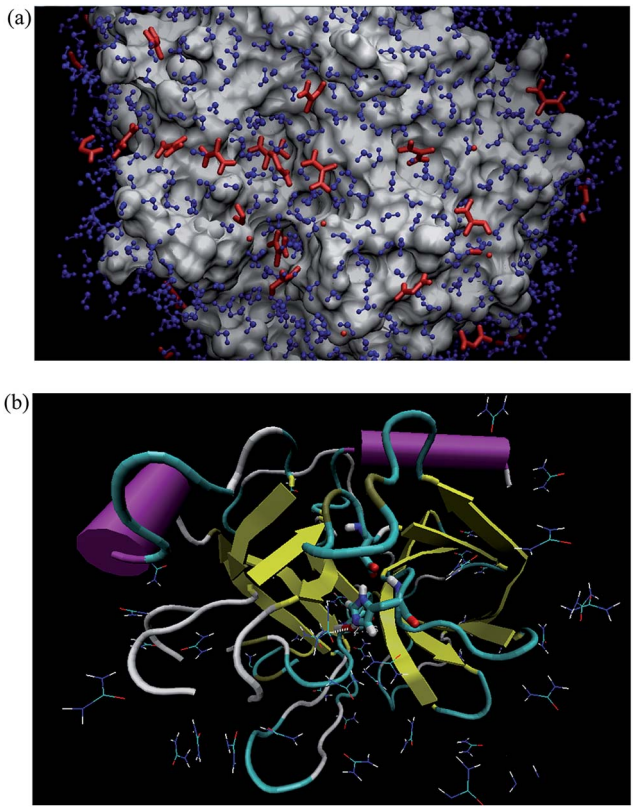

Fig. 14 (a) Urea molecules locate within 0.5 nm of protein surface. (b) The hydrogen bond formation between (UREA:H···SER195:OG).

stabilizers. In addition, our results are in good agreement with MD simulation studies, in which stabilizer enhances the tetrahedral water structure and weakens the interactions between protein functional groups and water molecules, which leads to protect protein native structure.[74,79 82] In other words, our results strongly suggest that urea (or) GdnHCl effectively disrupts the native structure of trypsin *via* preferential binding. Interestingly, our findings are in agreement with existing results from molecular dynamic simulations[83 87] as well as the experimental results.[15,19,28,88,89] Obviously, it appears that GdnHCl, urea, betaine, proline and TMAO do affect different forms of structure in distinctly different ways, from both molecular and structural tandpoints. Further research needs to be performed on trypsin carp along with trypsin from other carps and common carp to see how other proteins handle osmotic stress as it is apparent that proteins from different species may be affected differently.

4. Conclusions

Trypsin was purified from the hepatopancreas of Indian major carp, Catla *C. catla* by fractional precipitation with ammonium sulfate and was followed with ion exchange and affinity chromatography. SDS-PAGE of purified trypsin PF2, of Indian major carp Catla, revealed a homogenous single band with molecular mass of 19.72 kDa. A 107.4 fold purification of trypsin was observed from the purification of trypsin from Catla, with the yield of 24.6%. Purified enzyme from Catla was completely inhibited by soybean trypsin inhibitor (SBTI) and specific trypsin inhibitor (TLCK). Activity bands were significant in substrate SDS-PAGE (zymogram). The stabilizer or denaturant-induced structural alteration of trypsin was studied by monitoring the UV-Vis, fluorescence and thermal fluorescence and CD measurements. To ensure our experimental results, we further studied MD simulation using GROMACS 4.5.5 package. It was concluded that the native structure of trypsin was stabilized in the presence of osmolyte tend to exclude from the enzyme surface, forcing the polypeptide to adopt a compactly folded structure. The trypsin structure starts denaturing with increasing concentration of urea or GdnHCl and reaches a completely unfolded state due to the preferentially binding. Moreover, our results vividly demonstrated that betaine exerts a powerful stabilizer and most effective compatible osmolyte, whereas TMAO is a weak stabilizer and least protective osmolyte. The structure and function of trypsin was strongly influenced by the cosolvent through biomolecular interaction between the vicinity of protein surface and the co-solvents. Our results reveal that the preferential interactions occur between the surface of trypsin and neighbouring particles of co-solvents through exclusion of osmolyte or inclusion of denaturant. The wide range of applications of co-solvents will continue to improve with the advent of new biological applications providing novel information in the field of protein stability research.

Acknowledgements

We gratefully acknowledge the Council of Scientific Industrial Research (CSIR), New Delhi, Department of Science and Technology (DST), New Delhi, Department of Biotechnology (DBT), New Delhi through the grant no. 01(2713)/13/EMR-II, SB/S1/PC-109/2012, no. BT/PR5287/BRB/10/1068/2012, respectively for financial support.

References

1 S. Klomklao, S. Benjakul, W. Visessanguan, H. Kishimura and B. K. Simpson, *J. Agric. Food Chem.*, 2006, **54**, 5617–5622.
2 S. Klomklao, S. Benjakul, W. Visessanguan, H. Kishimura and B. K. Simpson, *Food Chem.*, 2007, **100**, 1580–1589.
3 E. Toyota, D. Iyaguchi, H. Sekizaki, K. Itoh and K. Tanizawa, *Biol. Pharm. Bull.*, 2007, **30**, 1648–1652.
4 N. F. Haard, *J. Aquat. Food Prod. Technol.*, 1992, **1**, 17–35.
5 M. Macouzet, B. K. Simpson and B. H. Lee, *Fed. Eur. Microbiol. Soc. Microbiol. Lett.*, 2005, **5**, 851–857.
6 B. K. Simpson, *Digestive Proteases from Marine Animals*, Academic Press, Inc. New York, 2000.
7 S. De Vecchi and Z. Coppes, *J. Food Biochem.*, 1996, **20**, 193–214.
8 P. H. Yancey, M. E. Clarke, S. C. Hand, R. D. Bowlus and G. N. Somero, *Science*, 1982, **217**, 1214–1222.
9 G. N. Somero, *Annu. Rev. Physiol.*, 1995, **57**, 43–68.
10 S. Ortiz-Costa, M. M. Sorenson and M. Sola-Penna, *FEBS J.*, 2008, **275**, 3388–3396.

11 S. Ortiz-Costa, M. M. Sorenson and M. Sola-Penna, *Arch. Biochem. Biophys.*, 2002, **408**, 272–278.
12 G. A. Spitz, C. M. Furtado, M. Sola-Penna and P. Zancan, *Biochem. Pharmacol.*, 2009, **77**, 46–53.
13 A. Kumar and P. Venkatesu, *Chem. Rev.*, 2012, **112**, 4283–4307.
14 P. Venkatesu, M. J. Lee and H. M. Lin, *J. Phys. Chem. B*, 2009, **113**, 5327–5338.
15 P. Venkatesu, M. J. Lee and H. M. Lin, *J. Phys. Chem. B*, 2007, **111**, 9045–9056.
16 P. Venkatesu, M. J. Lee and H. M. Lin, *Arch. Biochem. Biophys.*, 2007, **466**, 106–115.
17 P. Attri, P. Venkatesu and M. J. Lee, *J. Phys. Chem. B*, 2010, **114**, 1471–1478.
18 T. O. Street, D. W. Bolen and G. D. Rose, *Proc. Natl. Acad. Sci. U. S. A.*, 2006, **103**, 13997–14002.
19 R. C. Diehl, E. J. Guinn, M. W. Capp, O. V. Tsodikov Jr and M. T. Record, *Biochemistry*, 2013, **52**, 5997–6010.
20 D. Wu and A. P. Minton, *J. Phys. Chem. B*, 2013, **117**, 9395–9399.
21 R. Jain, D. Sharma, S. Kumar and R. Kumar, *Biochemistry*, 2014, **53**, 5221–5235.
22 D. R. Canchi and A. E. García, *Annu. Rev. Phys. Chem.*, 2013, **64**, 273–293.
23 A. Rani and P. Venkatesu, *Int. J. Biol. Macromol.*, 2015, **73**, 189–201.
24 Y. L. Shek and T. V. Chalikian, *Biochemistry*, 2013, **52**, 672–680.
25 G. Graziano, *Phys. Chem. Chem. Phys.*, 2011, **13**, 17689–17695.
26 A. Wang and D. W. Bolen, *Biochemistry*, 1997, **36**, 9101–9108.
27 J. Hunger, N. Ottosson, K. Mazur, M. Bonn and H. J. Bakker, *Phys. Chem. Chem. Phys.*, 2015, **17**, 298–306.
28 A. Huerta-Viga and S. Woutersen, *J. Phys. Chem. Lett.*, 2013, **4**, 3397–3401.
29 T. Arakawa and S. N. Timasheff, *Biochemistry*, 1984, **23**, 5924–5929.
30 P. K. Nandi and D. R. Robinson, *Biochemistry*, 1984, **23**, 6661–6668.
31 S. N. Timasheff and G. Xie, *Biophys. Chem.*, 2003, **105**, 421–448.
32 E. Sherman and G. Haran, *Proc. Natl. Acad. Sci. U. S. A.*, 2006, **103**, 11539–11543.
33 C. P. Schneider and B. L. Trout, *J. Phys. Chem. B*, 2009, **113**, 2050–2058.
34 B. K. Khangembam, Y. V. R. K. Sharma and R. Chakrabarti, *Int. Aquatic Res.*, 2012, **4**, 1–12.
35 B. F. Erlanger, N. Kokowsky and W. Cohen, *Arch. Biochem. Biophys.*, 1961, **95**, 271–278.
36 U. K. Laemmli, *Nature*, 1970, **277**, 680–685.
37 J. Walter, W. Steigemann, T. P. Singh, H. Bartunik, W. Bode and R. Huber, *Acta Crystallogr., Sect. B: Str*, 1982, **38**, 1462–1472.
38 R. Anandakrishnan, B. Aguilar and A. V. Onufriev, *Nucleic Acids Res.*, 2012, **40**, W537–W541.
39 D. Van Der Spoel, E. Lindahl, B. Hess, G. Groenhof, A. E. Mark and H. J. C. Berendsen, *J. Comput. Chem.*, 2005, **26**, 1701–1718.
40 C. Oostenbrink, A. Villa, A. E. Mark and W. F. Van Gunsteren, *J. Comput. Chem.*, 2004, **25**, 1656–1676.
41 L. J. Smith, R. M. Jones and W. F. van Gunsteren, *Proteins: Struct., Funct., Bioinf.*, 2005, **58**, 439–449.
42 C. Camilloni, A. Guerini Rocco, I. Eberini, E. Gianazza, R. A. Broglia and G. Tiana, *Biophys. J.*, 2008, **94**, 4654–4661.
43 A. K. Malde, L. Zuo, M. Breeze, M. Stroet, D. Poger, P. C. Nair, C. Oostenbrink and A. E. Mark, *J. Chem. Theory Comput.*, 2011, **7**, 4026–4037.
44 H. J. C. Berendsen, J. R. Grigera and T. P. Straatsma, *J. Phys. Chem.*, 1987, **91**, 6269–6271.
45 M. Taha, B. S. Gupta and M. J. Lee, *J. Chem. Eng. Data*, 2011, **56**, 3541–3551.
46 L. Alderighi, P. Gans, A. Ienco, D. Peters, A. Sabatini and A. Vacca, *Chem. Rev.*, 1999, **184**, 311–318.
47 T. Darden, D. York and L. Pedersen, *J. Chem. Phys.*, 1993, **98**, 10089–10092.
48 B. Hess, *J. Chem. Theory Comput.*, 2007, **4**, 116–122.
49 G. Bussi, D. Donadio and M. Parrinello, *J. Chem. Phys.*, 2007, **126**, 014101–014107.
50 M. Parrinello and A. Rahman, *J. Appl. Phys.*, 1981, **52**, 7182–7190.
51 W. Humphrey, A. Dalke and K. Schulten, *J. Mol. Graphics*, 1996, **14**, 33–38.
52 V. Baldwin, M. Bhatia and M. Luckey, *Biochim. Biophys. Acta*, 2011, **1808**, 2206–2213.
53 S. E. Bondos and A. Bicknell, *Anal. Biochem.*, 2003, **316**, 223–231.
54 A. H. Dewald, J. C. Hodges and L. Columbus, *Biophys. J.*, 2011, **100**, 2131–2140.
55 E. S. Courtenay, M. W. Capp and M. T. Record Jr, *Protein Sci.*, 2001, **10**, 2485–2497.
56 G. Graziano, *Phys. Chem. Chem. Phys.*, 2010, **12**, 14245–14252.
57 C. N. Pace and D. V. Laurents, *Biochemistry*, 1989, **28**, 2520–2525.
58 P. L. Privalov, *Adv. Protein Chem.*, 1979, **33**, 167–241.
59 P. Bruzździak, A. Panuszko and J. Stangret, *J. Phys. Chem. B*, 2013, **117**, 11502–11508.
60 T. Arakawa and S. N. Timasheff, *Arch. Biochem. Biophys.*, 1983, **224**, 169–177.
61 T. Arakawa and S. N. Timasheff, *Biophys. J.*, 1985, **47**, 411–414.
62 A. K. Mandal, S. Samaddar, R. Banerjee, S. Lahiri, A. Bhattacharyya and S. Roy, *J. Biol. Chem.*, 2003, **278**, 36077–36084.
63 M. M. Santoro, Y. Liu, S. M. A. Khan, L. X. Hou and D. W. Bolen, *Biochemistry*, 1992, **31**, 5278–5283.
64 V. L. Brewster, L. Ashton and R. Goodacre, *Anal. Chem.*, 2013, **85**, 3570–3575.
65 X. Hu, Z. Yu and R. Liu, *Spectrochim. Acta, Part A*, 2013, **108**, 50–54.
66 I. M. Kuznetsova, T. A. Yakusheva and K. K. Turoverov, *FEBS Lett.*, 1999, **452**, 205–210.
67 W. Qiu, T. Li, L. Zhang, Y. Yang, Y. T. Kao and L. Wang, *Chem. Phys.*, 2008, **350**, 154–164.

68 P. D. Adams, Y. Chen, K. Ma, M. G. Zagorski, F. D. Sonnichsen, M. L. McLaughlin and M. D. Barkley, *J. Am. Chem. Soc.*, 2002, **124**, 9278–9286.
69 Y. Chen and M. D. Barkley, *Biochemistry*, 1998, **37**, 9976–9982.
70 N. J. Greenfield, *Nat. Protoc.*, 2006, **1**, 2527–2535.
71 S. M. Kelly, T. J. Jess and N. C. Price, *Biochim. Biophys. Acta*, 2005, **1751**, 119–139.
72 L. M. Simon, M. Kotorman, A. Szabo and A. Garab, *Biochem. Biophys. Res. Commun.*, 2004, **317**, 610–613.
73 P. Bruździak, A. Panuszko and J. Stangret, *J. Phys. Chem. B*, 2013, **117**, 11502–11508.
74 D. R. Canchi, P. Jayasimha, D. C. Rau, G. I. Makhatadze and A. E. Garcia, *J. Phys. Chem. B*, 2012, **116**, 12095–12104.
75 R. S. Phillips, A. K. Wang, S. Marchal and R. Lange, *Biochemistry*, 2012, **51**, 9354–9363.
76 J. Seeliger, K. Estel, N. Erwin and R. Winter, *Phys. Chem. Chem. Phys.*, 2013, **15**, 8902–8907.
77 T. R. Silvers and J. K. Myers, *Biochemistry*, 2013, **52**, 9367–9374.
78 H. Kokubo, C. Y. Hu and B. M. Pettitt, *J. Am. Chem. Soc.*, 2011, **133**, 1849–1858.
79 S. Hwang, Q. Shao, H. Williams, C. Hilty and Y. Q. Gao, *J. Phys. Chem. B*, 2011, **115**, 6653–6660.
80 E. A. Mills and S. S. Plotkin, *J. Phys. Chem. B*, 2013, **117**, 13278–13290.
81 J. Rösgen and R. Jackson-Atogi, *J. Am. Chem. Soc.*, 2012, **134**, 3590–3597.
82 N. Kumar and N. Kishore, *J. Chem. Phys.*, 2013, **139**, 115104–115109.
83 J. L. England, V. S. Pande and G. Haran, *J. Am. Chem. Soc.*, 2008, **130**, 11854–11855.
84 J. Almarza, L. Rincon, A. Bahsas and F. Brito, *Biochemistry*, 2009, **48**, 7608–7613.
85 B. Moeser and D. Horinek, *J. Phys. Chem. B*, 2014, **118**, 107–114.
86 U. D. Priyakumar, C. Hyeon, D. Thirumalai and A. D. MacKerell, *J. Am. Chem. Soc.*, 2009, **131**, 11759–11761.
87 A. Caballero-Herrera, K. D. Nordstrand, K. D. Berndt and L. Nilsson, *Biophys. J.*, 2005, **89**, 842–857.
88 J. K. Chung, M. C. Thielges, S. R. Lynch and M. D. Fayer, *J. Phys. Chem. B*, 2012, **116**, 11024–11031.
89 I. M. Pazos and F. Gai, *J. Phys. Chem. B*, 2012, **116**, 12473–12478.